Journal of
Synchrotron
Radiation

ISSN 0909-0495

Received 13 December 2006
Accepted 26 March 2007

Beam-size-related phenomena and effective normalization in energy-dispersive EXAFS for the study of heterogeneous catalysts, powder materials and the processes they mediate: observations and (some) solutions

Mark A. Newton

European Synchrotron Radiation Facility, 6 Rue Jules Horowitz, BP 220, Grenoble, France.
E-mail: newton@esrf.fr

The effects of focal spot size and the nature of powder samples (such as heterogeneous catalysts) on the quality of data obtainable from a dispersive EXAFS experiment are characterized at ID24 of the ESRF. Using examples of supported Pd catalysts, it is shown that, for a given photon flux, massive improvements in data quality can be achieved by increasing the size of the dispersive beam in the vertical, whilst concurrently applying a methodology to account for scattering effects emanating from the samples under study. These improvements are demonstrated using progressively practical and demanding examples. Questions regarding optimal beam dimensions for the study of such materials, how to counter undesirable effects that arise from the coherence of the source, how to obtain similar results consistently across the 5–30 keV bandwidth of ID24, and whether a methodology for simultaneous normalization in dispersive EXAFS is of significant utility in such circumstances are discussed.

Keywords: energy-dispersive EXAFS; time-resolved XAFS; heterogeneous catalysis; powders; material science; normalization; scattering; chemical processes.

1. Introduction

Of the family of X-ray absorption fine-structure (XAFS) spectroscopies, energy-dispersive EXAFS (EDE) (Matsushita & Phizackerley, 1981) has always held great promise for studying fast processes from a local structure point of view; specifically through the acquisition of EXAFS data, as well as XANES, on time scales significantly less than 1 s and in a single shot. This is possible as the EDE experiment comprises no moving parts, and the energetic bandwidth required to obtain EXAFS may be applied to a sample instantaneously, rather than requiring a stepwise approach to obtaining data over the required energy range. The optical arrangement is also therefore intrinsically stable and produces inherently small beam foci ($\ll$500 µm × 500 µm).

These properties have also imbued the technique with a great potential for application in other areas, most notably high-pressure physics (Fontaine *et al.*, 1992; Perlin *et al.*, 1992; Sapelkin *et al.*, 2000; Pascarelli *et al.*, 2006; Aquilanti & Pascarelli, 2005), magnetic dichroism (Baudelet *et al.*, 1997; Fontaine *et al.*, 1992; Mathon *et al.*, 2004), differential EXAFS (Pettifer *et al.*, 2005) and, most recently, mapping at high spatial resolutions (Pascarelli *et al.*, 2006; Muñoz *et al.*, 2006). As such, the developmental tendency has been towards the smaller and more brilliant focal spots required for this sort of research. Indeed, a recent paper (Pascarelli *et al.*, 2006) has nicely delineated this historical improvement. To summarize, ID24 has seen a diminution in the horizontal size of the focal spot by over an order of magnitude (to $<$5 µm up to 15 keV). With the implementation of a new first mirror the vertical height of the beam has also been reduced considerably and provides (at full focus) a beam height of $\sim$100 µm. This may be further reduced through the addition of a further focusing mirror in the experimental hutch itself to yield focal spots of 5 µm × 5 µm.

Heterogeneous catalysts (and any form of powder sample) are, by their very nature, spatially non-homogeneous. They are also often comprised of very small quantities ($\ll$5 wt%) of the element of interest for structural study, and supported upon a dispersant that comprises other heavy elements (for instance, Ce and Zr amongst others) that may scatter X-rays and otherwise interfere with the task of obtaining reliable structural information. Moreover, from the point of view of a catalytic process, other parameters must be considered that further place constraints on the experiment. For example, plug flow conditions, wherein all the gaseous feedstock must pass

through the entire sample bed and one can define the feedstock space velocity (flow rate/catalyst volume), are ideally required. Within this paradigm the allowable sample particle size required to permit an even mass flow throughout the sample is constrained by the dimensions of the bed itself: too large and gas bypassing effects at the reactor walls will nullify the plug flow nature of the system; too small and 'clogging' will overly restrict gas flows, accessible space velocities, and lead to back pressure problems (Satterfield, 1996).

As such, the successful application of XAFS to produce meaningful and new insights into the structural reactive dynamics of such systems, and the processes they facilitate, pose a number of potential problems that need to be considered and overcome. As has been pointed out, to make an EXAFS measurement or a reactivity measurement is (nowadays) relatively facile. To construct an experiment that does both in a meaningful manner at the same time is considerably more problematic (Bare *et al.*, 2007); despite its clear potential, EDE presents more hurdles to overcome in these respects, one could argue, than any other XAFS variant.

This is because the unique nature of the dispersive approach, as well as bringing unique possibilities, also brings problems and limitations specific to it. Prime amongst these are the inability to obtain a synchronous normalization of the absorption data, and an extreme requirement for spatial homogeneity within the sample under study. Furthermore, a pure dispersive experiment does not permit fluorescence yield detection.

Fluorescence detection is possible using dispersive optics in the so-called 'turbo' approach (Pascarelli *et al.*, 1999). However, to permit this, a moving element is introduced to the system (a slit that traverses the beam) and XAFS is collected in a stepwise manner as in traditional EXAFS techniques. This approach has recently found practical application in the study, at the Pt L_{III}-edge, of commercial auto-exhaust catalysts on the time scale of $\sim$1 s.[1] The combination of low levels of Pt (0.5–2 wt%) and high levels of heavy scatterers within the support material in such catalysts makes a traditional transmission experiment very difficult. However, whilst the turbo approach has proved successful in allowing some time-resolved studies to be made, and is the subject of current augmentation,[2] only XANES has thus far been achieved on these time scales.

This paper aims to build on some previous studies and observations, notably those of Hagelstein *et al.* (1998) and Newton *et al.* (2006*a*,*b*,*c*), and tries to start to critically assess and quantify the parameters that are of most importance in taking the potential of the pure transmission-based EDE experiment and turning it into some form of EXAFS reality for the dynamic study of heterogeneous catalyst systems and processes involving powder samples in general. It will be shown that the empirical understanding that arises can be directly translated into a very significant augmentation of the performance of the technique for such studies. Lastly, it will become clear that the drive for the smaller and smaller spot sizes required to suit the needs of high-pressure studies, and micrometer-level mapping experiments, have a tendency to make the energy-dispersive approach technique progressively less compatible with the sorts of materials, and the manner in which they may be meaningfully studied, that are extensively researched within a range of important disciplines wherein heterogeneous catalysis is but one.

[1] Proprietary research undertaken on ID24 by the Toyota Motor Corporation.
[2] An augmentation of the turbo approach, currently under development at the ESRF, is to replace the current slit (that traverses the beam in a one-dimensional manner) with a rotating (spiral) slit. Such a slit should provide the capacity for continuous data collection, reducing dead-time in the acquisition process. Given adequate S/N (signal-to-noise ratio), it is foreseen that fluorescence yield XANES on the 10 Hz time scale and EXAFS at 1 Hz should be achievable.

2. Experimental

The studies presented here were conducted in the 2/3 mode of filling utilized at the ESRF yielding a maximal 200 mA current. The beamline layout of ID24 has been well described elsewhere (Pascarelli *et al.*, 2006) but, to summarize, the studies were made at the Pd *K*-edge (24.35 keV) using a single U42 undulator at the fifth harmonic and utilizing the Pt-coated stripes on the two mirrors prior to the polychromator (Pascarelli *et al.*, 2006). The polychromatic and focused X-ray beam was produced using a symmetrically cut Si [311] polychromator in Bragg configuration. At the Pd *K*-edge this produces a focal spot with a horizontal FWHM of $\sim$100–150 µm; vertically, when the first mirror is fully focused, a beam height of $\sim$100 µm results. The EDE was measured in transmission using a 16-bit FReLoN camera (Labiche *et al.*, 2007).

Supported Pd samples (at 4 wt% and 1 wt% Pd loading), synthesized as described elsewhere (Iglesias-Juez *et al.*, 2004, 2005; Fernández-García *et al.*, 2001), were mounted in a cell designed for synchronous EDE/diffuse reflectance infrared spectroscopy (DRIFTS)/mass spectrometric studies of working catalysts [this cell being based upon a commercially available DRIFTS system (Spectratech) and a development of that published elsewhere (Newton *et al.*, 2004, 2006*b*,*c*, 2007). Samples were sieved to a 80–112 µm fraction before use and loaded into the cell with an effective bed density (mass of sample/bed volume) of $\leq$1 g cm^{-3}. The sample bed is comprised of a 5 mm internal diameter BN ring (0.2 mm wall thickness; 2.5 mm height) mounted upon a stainless-steel mesh of nominal 40 µm aperture diameter. The sample sits upon the heating element and the feedstocks to be flowed over the sample pass through the bed of material and down the centre of the heater. This arrangement therefore has within it the basic requirements of plug flow study, whilst permitting DRIFTS and transmission-based X-ray experiments with equanimity. For transmission of the X-rays, two polished 5 mm-diameter $\times$ 1 mm-thick vitreous carbon windows (Sigradur) have also been added to this cell. Lastly, the set-up also permits the mounting of a second BN sample mount, at the same focal length as the sample, outside the environmental cell itself.

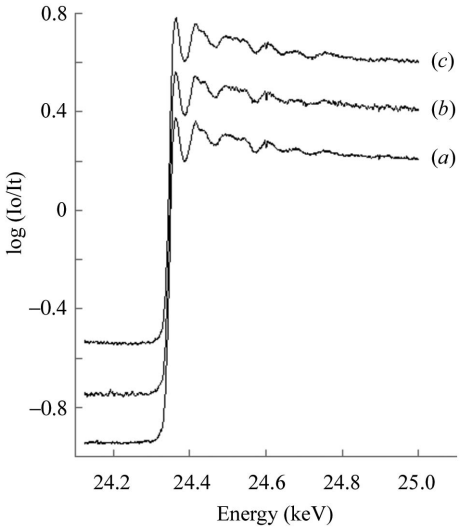

Figure 1
Raw dispersive EXAFS spectra derived from a 4 wt% Pd/Al_2O_3 sample at room temperature under flowing He (75 ml min^{-1}) as a function of vertical beam height (VBH): (*a*) under-bending the mirror to a VBH of 260 μm; (*b*) VBH at ideal focus = 100 μm; (*c*) over-bending of the mirror to yield a beam height of 300 μm. The net acquisition time is 100 ms for each spectrum (25 frames × 4 ms integration time). The reference is a passage through air.

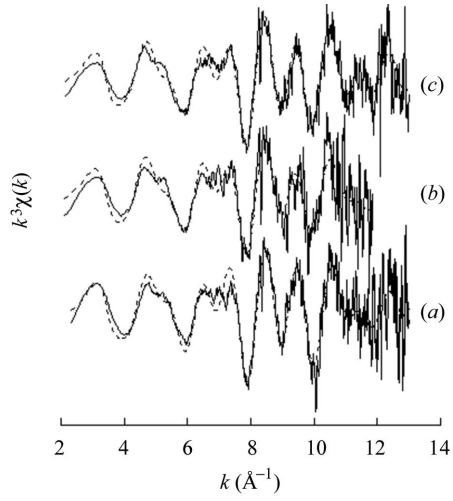

Figure 2
k^3-Weighted EXAFS spectra derived from 4 wt% Pd/Al_2O_3 in 100 ms as a function of vertical beam size: (*a*) under-bending the mirror to a VBH of 260 μm; (*b*) VBH at ideal focus = 100 μm; (*c*) over-bending of the mirror to yield a beam height of 300 μm. Dashed lines are from theoretical fitting using *EXCURV*.

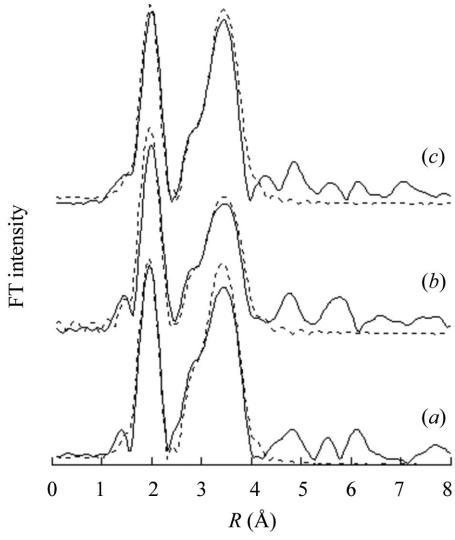

Figure 3
Fourier transform (FT) representations of the data shown in Figs. 1 and 2. Again, (*a*) under-bending the mirror to a VBH of 260 μm; (*b*) VBH at ideal focus = 100 μm; (*c*) over-bending of the mirror to yield a beam height of 300 μm. Dashed lines are from theoretical fitting using *EXCURV*.

3. Results

3.1. Effects of the vertical size of the X-ray beam

The horizontal dimension of the X-ray beam at the focal spot, arising from the bending of a Bragg or Laue Si single-crystal, is not variable. In this respect, therefore, the only accessible variable is in the vertical dimension. In standard operation the first beamline mirror is bent to focus at the position of the X-ray detector. As such we may manipulate the vertical beam height (VBH) by over- or under-bending this mirror.

The results of doing this, on the raw absorption data obtained in 100 ms (50 frames × 2 ms) from 4% Pd/Al_2O_3 for three values of the VBH [focused; ∼100 μm under-bent (to ∼260 μm); over-bent (to ∼300 μm), as indicated] are shown in Fig. 1. The resulting k^3-weighted EXAFS and Fourier transform representations of the data are shown in Figs. 2 and 3, respectively. Table 1 summarizes the structural and statistical parameters derived from analysis of the EXAFS using *PAXAS* (Binsted, 1988) and *EXCURV* (Binsted, 1998) along with those derived from a bulk PdO spectrum derived from a standard scanning EXAFS experiment analysed to the same data length.

It is clear that the quality of the data obtained from the dispersive experiment is a significant function of the VBH (most clearly in the raw absorbance and *k*-weighted forms). Indeed, the worst situation is seen to occur when the beam is focused; progressive over- or under-bending of the mirror results in progressively better data.

From a structural point of view it is clear that in this state the Pd is in a predominantly nanoparticulate form of PdO. The fitting here is not exhaustive and more detailed assessments will appear elsewhere. The refinement fixes the expected shell progression and occupancy from bulk PdO whilst fitting with only the Debye–Waller (DW) factor, Fermi energy (E_F) and the shell radii (R). As such, the shell occupancies cannot be considered 'real'.

The above measurements all utilized a simple unobstructed path through air as the reference measurement. This represents the simplest and most often used approach to normalization in dispersive measurements. This approach implicitly assumes that the sample itself does not modify the beam in any

Table 1
Structural and statistical parameters extracted from analysis (using *PAXAS* and *EXCURV*) of the EDE data shown in Figs. 1 and 2 from 4 wt% Pd/Al_2O_3 samples and from a standard PdO bulk reference spectrum (all at 300 K).

In these analyses the shell occupations are fixed whilst the Debye–Waller (DW) factors, bond lengths (R) and Fermi energy (E_F) are refined. CN = coordination number.

VBH (mm)	k_{min} (Å^{-1})	k_{max} (Å^{-1})	Scatterer	CN	R (Å^{-1})	DW ($2\sigma^2$)	E_F (eV)	R (%)
300	2	13.00	O	4	2.01	0.007	2.7	44
			Pd	4	3.01	0.014		
			Pd	8	3.41	0.013		
100	2	13.00	O	4	2.01	0.006	2.5	69.7
			Pd	4	3.00	0.015		
			Pd	8	3.42	0.016		
260	2	13.00	O	4	2.00	0.007	4.5	52.9
			Pd	4	3.00	0.013		
			Pd	8	3.41	0.014		
Bulk PdO	2	13.00	O	4	2.029	0.007	3.7	37.4
			Pd	4	3.056	0.007		
			Pd	8	3.445	0.014		

way except for the absorption due to the element under study. This is clearly a highly simplistic view of affairs, especially when the sample is a powder, the intrinsic coherence of the beam is high, the spectrum obtained from a two-dimensional image, and one is constrained to work in transmission.

In this first case the variations in obtained data quality do not prevent a Pd phase identification. It is clear, however, even in this relatively facile case, that the 'certainty' of any such determination, and the structural detail that is reasonably accessible, are very dependent on the VBH. One can easily imagine (and indeed this will be shown) that, if one carried the base level of data quality obtained in the worst case (focused first mirror; VBH $\sim$100 µm) into a much more challenging situation, one would have little chance of performing a successful EXAFS experiment.

3.2. Effects of the reference (I_o) measurement

Heavy elements (such as Ce and Zr) are omnipresent within the formulation of modern commercial automotive exhaust catalysts, and it is well known that these can cause problems in transmission-based EXAFS studies through their capacity for absorbing/scattering the X-rays as they pass through such samples. In a standard scanning EXAFS experiment, inelastic scattering and absorption manifest themselves primarily in a steeply rising background that complicates the extraction of the EXAFS. This is especially so when the element under study is present in small amounts and the resulting edge jump is small. In such cases, fluorescence yield often becomes the preferred method of detection as these effects can often be more effectively minimized than in a standard transmission experiment.

In the pure dispersive EXAFS experiment this situation is further complicated. In addition to this sort of inelastic scattering effect, the experiment becomes sensitive to elastic small-angle scattering (SAXS) which will pass, unavoidably, straight into the spatially resolving detection system. The high coherence of the source exacerbates this problem. The existence and problematic nature of these effects on ID24 was noted some years ago (Hagelstein *et al.*, 1998) in considering the XANES structure of Pt samples at the L_{III}-edge. The solution of Hagelstein *et al.* was to introduce a scattering filter system, comprised of two channel-cut Si(220) crystals before and after the sample, in the so-called Bonse–Hart camera configuration (Bonse & Hart, 1965). Whilst this appeared to work well for the XANES problems that were being studied at the time, this particular approach has seen no further implementation. As will become clear, however, a further assessment of the utility and practicability of this approach for lower-energy EXAFS studies would seem warranted.

Unfortunately, practically any sample material will also scatter the transmitted X-ray beam in this sort of manner to a greater or lesser degree. Moreover, it is the case that a good many commercial catalysts/materials of technological interest utilize elements/dispersants that are, in themselves, rather good small-angle scatterers, in tandem with low (1 wt% or less) loadings of the precious metals that are generally the subject of interest in their study using EXAFS techniques.

Having shown that the dimensions of the beam appear to be directly related to the quality of data one can achieve at a relatively high loading of 4 wt% Pd, we now move to a considerably more challenging situation in order to investigate how effective an adequate reference material can be. The results shown in Figs. 4, 5 and 6 are derived from samples containing only 1 wt% Pd and supported upon an Al_2O_3 dispersant containing 10 wt% CeZr (10ZCA). This support is about a factor of three to four times as absorbing as Al_2O_3 at the Pd K-edge and roughly an order of six to eight times as absorbing as the corresponding passage through air.

Fig. 4 shows the raw absorption data, Fig. 5 shows the k^3-weighted EXAFS, and Fig. 6 shows the corresponding Fourier transform (FT) representations. These data were taken sequentially using equivalent acquisition times (100 ms) and with no change to the configuration of the beamline (except for a change in the focus of the first mirror) or detector. Fig. 7 (raw absorption data), Fig. 8 (k^3-weighted EXAFS) and Fig. 9 (FT representation) show the effect of increasing the net acquisition to $\sim$1 s, whilst using the 10ZCA support material as the reference, and changing the VBH.

It can now be seen how much of a pivotal role the use of a suitable reference material is in these sorts of experiments. Whereas a simple enlargement of the VBH largely ameliorates the deleterious structure within the EXAFS derived from a 4 wt% Pd on Al_2O_3, this approach alone fails miserably from an EXAFS point of view (Fig. 4, spectrum *a*) when trying the same experiment with a 1 wt% loading of Pd supported upon a more absorbing/scattering support (10ZCA). One can still see that vertical enlargement of the beam does improve the data that can be obtained, relative to the case where the beam is still focused (on going from spectrum *a* to spectrum *b*). However, the EXAFS data length, crucial to any reliable/extensive analysis, that can be obtained is very restricted and at best, in this case, is about 8 Å^{-1}, even at 300 K.

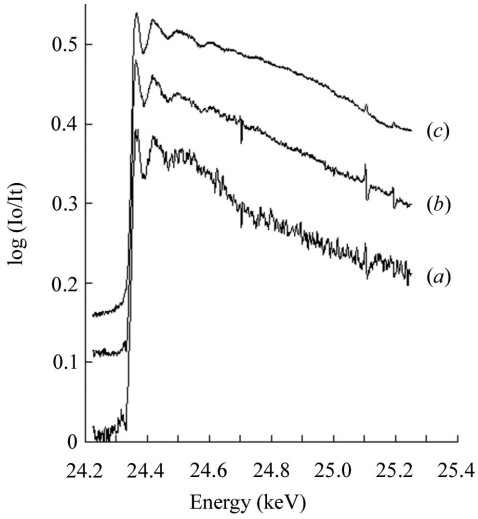

Figure 4
Raw EDE absorbance spectra derived from a 1 wt% Pd/10ZCA sample in 100 ms. (*a*) VBH = 100 µm, air reference; (*b*) VBH = 300 µm, air reference; (*c*) VBH = 300 µm, 10ZCA reference.

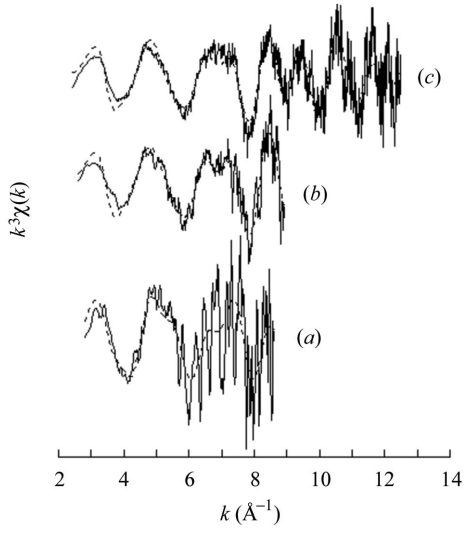

Figure 5
k^3-Weighted EXAFS spectra from the spectra shown in Fig. 4(*a*). (*a*) VBH = 100 µm, air reference; (*b*) VBH = 300 µm, air reference; (*c*) VBH = 300 µm, 10ZCA reference. Dashed lines are from theoretical fitting using *EXCURV*.

By utilizing a reference that now seeks to mimic that of the sample as closely as can be achieved in terms of a number of variables (such as composition, preparation, sieve fraction, sample bed density), a considerable transformation is achieved (spectrum *c*). Not only is there an improvement in the absolute S/N achieved under the same conditions, but the improvement in the normalization (in terms of the background and diminution of glitches) extends the obtainable data length to 12.5*k* at 100 ms acquisition time.

Part of this improvement comes simply from the fact that the use of the 10ZCA material as a reference effectively allows us to use more of the flux available to us on ID24 within the dynamic range of the detector system. As stated above, the 10ZCA is about six to eight times more absorbing than a

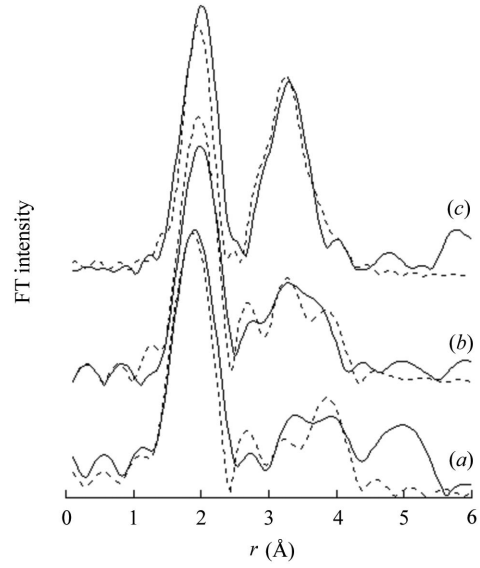

Figure 6
The corresponding FT representations of the data shown in Figs. 4 and 5. Again, (*a*) VBH = 100 µm, air reference; (*b*) VBH = 300 µm, air reference; (*c*) VBH = 300 µm, 10ZCA reference. Dashed lines are from theoretical fitting using *EXCURV*.

simple passage through air at the Pd *K*-edge; if it does nothing else, the introduction of a support reference material is helping us to fully exploit the available flux from the undulator-based ID24.[3] However, this alone, for equivalent net integration times, would only be expected to yield a statistical S/N improvement by a factor of about three at best.

The second, and in this case much more important, effect of the 'sample' reference is that it is much better at matching, and therefore accounting for, effects that are non-statistical in nature (such as the effects due to elastic and inelastic processes alluded to above). It is clear that the introduction of 10ZCA as the reference material leads to a much better overall shape of the absorbance spectra. Much more importantly, however, it effectively removes structure due to polychromator glitches and scattering from the support material itself.

That we have now arrived at a situation where we are no longer limited by non-statistical structure such as this is confirmed in Figs. 7 and 8. These also show that, whilst the variation of the vertical focus on its own cannot do much, in this particular case, to improve things, it is still required to obtain the best data when applied in tandem with the 'sample' reference; a tangible improvement in the k^3-weighted data can

[3] An alternative solution to the problem of utilizing more of the available photon flux within the bandwidth of the detector does exist and is already in place on ID24. This takes the form of an adjustable aperture ('iris') placed in between the phosphor screen and the detector chip itself. In principle, the size of this aperture can be varied for sample and reference measurements such that one is not limited (in the photon flux one can apply in the transmission experiment) by the (generally) less absorbing reference. However, it has been found that applying the existing 'iris' in this manner induces aberrations in the resulting spectra that make it currently unsuitable for systems of the type considered here. A non-aberrating aperture system for this application is currently being researched at the ESRF.

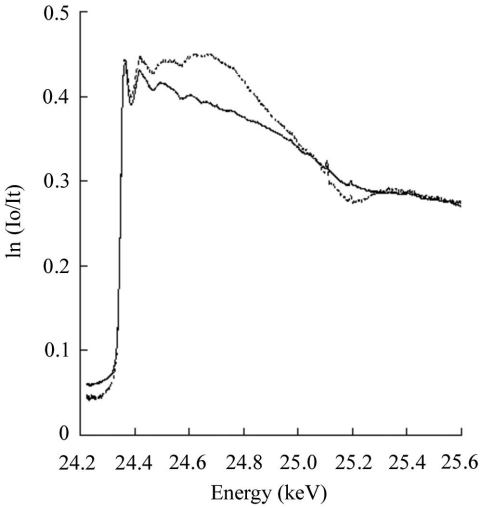

Figure 7
Raw EDE absorbance spectra derived from a 1 wt% Pd/10ZCA sample using 1 s of accumulation time. Solid line: VBH = 300 μm, 10ZCA reference. Dashed line: VBH = 100 μm, 10ZCA reference.

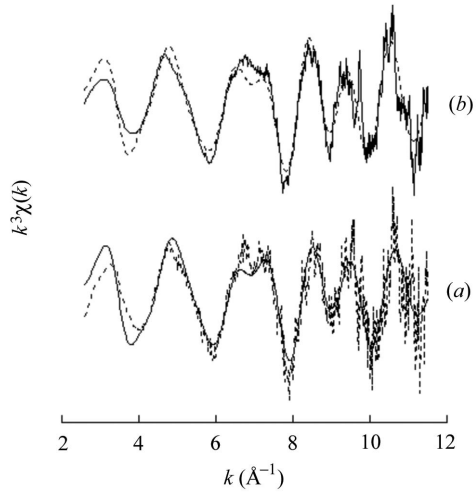

Figure 8
k^3-Weighted EXAFS spectra from the spectra shown in Fig. 7. (*a*) VBH = 100 μm, 10ZCA reference, (*b*) VBH = 300 μm, 10ZCA reference. Dashed lines are theoretical fits of the data from analysis using *EXCURV*.

be clearly seen between the two examples given in Fig. 8. However, it is also clear from Fig. 7 that obtaining the data shown in Fig. 8 is rather trickier when the beam VBH is reduced; the background subtraction and normalization of the data is obviously much more difficult, though, at least in this case, achievable. This is again related to the spatial homogeneity of the sample in the vertical direction. Defocusing the beam permits us to effectively average over the more local non-uniformities within the sample and therefore achieve a better extraction of the EXAFS.

3.3. Combining vertical beam enlargement and 'sample' normalization: a realistic process situation

In the above discussion we started with 4 wt% Pd/Al_2O_3 catalysts, and ended up with a capacity to obtain EXAFS from 1 wt% Pd/10ZCA samples from which extensive structural information may be restored on a 100 ms time scale. This, in itself, is a significant achievement, and has latterly put us in the upper operating regime of many commercial catalysts of this type in terms of Pd content. However, all of the above has been obtained at room temperature. Most catalytic processes work at considerably higher temperatures than this. As such, the techniques we have used to improve the performance of the experiment thus far must be demonstrated to not be compromised by this, or any other, requirement of the catalytic process.

Fig. 10 (raw absorption data), Fig. 11 (k^3-weighted EXAFS) and Fig. 12 (FT representation) show examples of how effective the implementation of the observations made above can be in a much more realistic and dynamic process situation. These show data derived from a 1 wt% Pd/10ZCA catalyst during switching between a reducing (5% CO/He) and oxidizing (5% NO/He) of the same flow rate (75 ml min^{-1}), at a temperature of 673 K.

In the current context it is sufficient to point out that such an experiment is considerably demanding from a dispersive

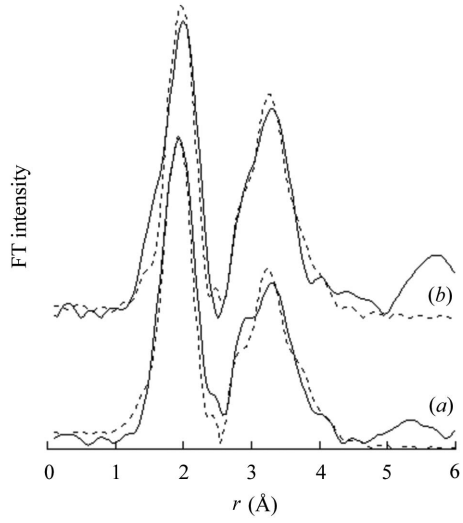

Figure 9
FT representation of the data shown in Figs. 7 and 8. (*a*) VBH = 100 μm, 10ZCA reference, (*b*) VBH = 300 μm, 10ZCA reference. Dashed lines are theoretical fits of the data from analysis using *EXCURV*.

EXAFS point of view: the loading of Pd is low and the bed lightly packed (with an effective bed density of ≤ 1 g cm^{-3}) to permit the required flow of gas without inducing significant back pressures; the support contains significant levels of heavy elements such as Ce and Zr; and the thermal component of the DW factor will be considerable for Pd at 673 K, leading to a significant attenuation of any EXAFS present.

Details of what may be derived from such an experiment, in terms of the structural reactive behaviour of the system under the process conditions being studied, will be given elsewhere (Newton, Belver *et al.*, 2007). However, Figs. 10, 11 and 12 show that even in this situation EXAFS can now be achieved (in this case at a repetition rate of 4 Hz) under these conditions. The combination of the nature of the sample and the temperature of investigation have naturally attenuated the length of the XAFS that may be achieved, but nonetheless

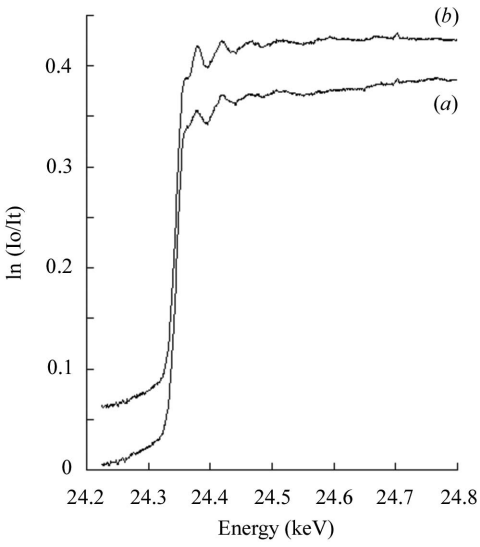

Figure 10
Raw EDE absorbance spectra derived from a 1 wt% Pd/10ZCA sample in 250 ms. (*a*) 1 wt% Pd/10ZCA sample under an initial 75 ml min^{-1} flow of He; (*b*) under 75 ml min^{-1} flow 5% CO/He. Spectra were taken during a cycling experiment between 75 ml min^{-1} 5% CO/He and 5% NO/He at 673 K.

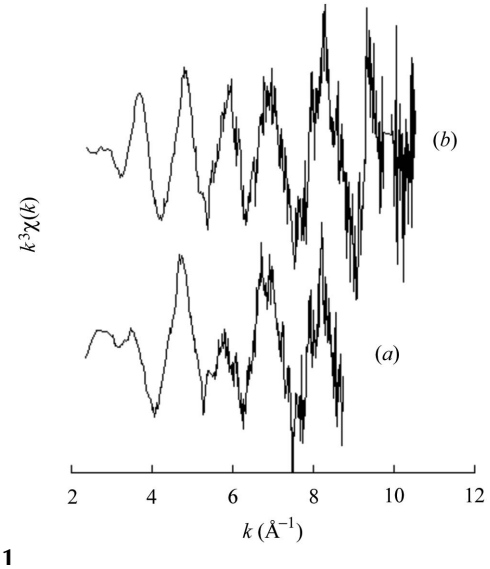

Figure 11
k^3-Weighted EXAFS spectra derived from the data shown in Fig. 10. (*a*) 1 wt% Pd/ZCA sample under an initial 75 ml min^{-1} flow of He; (*b*) under 75 ml min^{-1} flow 5% CO/He. Spectra were taken during cycling between 75 ml min^{-1} 5% CO/He and 5% NO/He at 673 K. In (*b*) the glitch present at ~24.7 keV in the raw absorption data (Fig. 10) has been removed prior to data reduction and analysis.

clearly structural information results. The Pd now has a nanoparticulate and largely metallic form [both Pd—Pd coordination and Pd—Pd bond lengths (from the FT representations) are indicative of this]. Under the inert He environment this phase retains a significant level of Pd—O coordination; in the reducing cycle of the experiment the Pd—O coordination is very much reduced and the Pd—Pd interaction at ~2.71 Å is tangibly increased; the shell integral derived from the FT in the range 2.2–3.1 Å has doubled. Although a more detailed analysis awaits (Newton, Belver *et al.*, 2007), to a first approximation the Pd sinters during the reducing (CO/He) cycle.

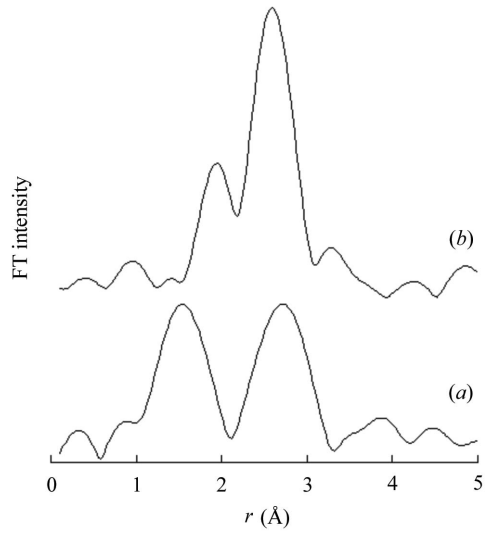

Figure 12
FT representations of the data shown in Figs. 10 and 11 (*a*) under He; (*b*) under 5% CO/He. Spectra were taken during cycling between 75 ml min^{-1} 5% CO/He and 5% NO/He at 673 K.

Importantly, this example shows that we have reached a position where we can study such fundamentally interesting and important systems and processes using dispersive EXAFS (rather than just XANES). Moreover, we can do this at high time resolution (250 ms in this case), low Pd loadings, and with other parameterization that, if not perfect, at least attempts to respect the nature of the chemical process in question.

4. Discussion

Considerable improvements in dispersive-EXAFS data from supported Pd catalysts can be achieved through manipulation of the vertical dimensions of the dispersive X-ray beam, matching the manner of sample presentation (net particle size and packing density) and the physical properties (composition, scattering ability) of the reference to that of the sample.

The improvements that can be achieved result predominantly from an increased ability to properly account for non-statistical structure emanating from the beamline optics (for instance, glitches inherent to the polychromator), and/or from the nature of the samples themselves. In addition, and particularly in the case of samples based upon highly absorbing support materials, this approach permits us to make a fuller use of the photon flux available at a third-generation undulator beamline, within the limitations of the dynamic range of the detector system.

In the cases considered here, that the reference material does not synchronously experience the gas flows and temperatures of a real catalytic experiment appears not to be relevant, even when the sample itself is experiencing a fluxional reactive environment at T = 673 K.

It has been shown that we can manipulate the vertical focus to considerably improve the performance of the technique for

obtaining EXAFS data. On ID24, and at the Pd *K*-edge, the intrinsic horizontal focus is at the large end of what is generally available from the symmetrically cut Bragg polychromators used (~100–150 μm FWHM). As such, when combined with a vertical beam enlargement (to 300 μm) we are utilizing a beam that covers $\sim 3 \times 10^4\ \mu m^2$. When convoluted with the pathlength of the transmission experiment and the approximate particle size of the sample, then as a rough estimate we are sampling of the order of 300 catalyst particles.

If we were to try the same experiment at the Pt L_{III}-edge, for example, a current symmetrically cut Bragg polychromator (as is in standard use on ID24) would produce a horizontal focus of $\lesssim 10$ μm. As such, in this case, and even with a vertical enlargement of the beam of the same type we have used here, we would only have a sampling area of $\sim 3 \times 10\ \mu m^2$. Further, at the Pt L_{III}-edge, the path length that can be reasonably utilized for a transmission experiment will also be somewhat curtailed, especially if the support is of an intrinsically absorbing nature. If we were to retain a similar net particle size with sample beds that were of the order of 1–3 mm in diameter, one would be reduced to sampling only somewhere between five and 20 catalyst particles.

Whilst a respect for plug flow conditions would require that the intrinsic particle size be reduced in proportion to the sample bed diameter [though only within certain bounds (Satterfield, 1996)], we can nonetheless anticipate, on the current evidence, that this decrease in the sampling volume of the experiment would be directly translated into a reduced data quality, given other conditions are the same, and a much higher susceptibility to the non-uniformity of the sample packing (leading to more difficult extraction of any EXAFS observed).

With the current undulator configuration of ID24, one could hypothetically make up in part the statistical side of the problem in terms of photon flux: it is possible to obtain more than ten times more photons at (for example) the Pt L_{III}-edge (11.564 keV) than at the Pd *K*-edge(24.35 keV).

However, it seems clear from the results presented here that the major problems that need to be overcome are not going to be ameliorated through a simple increase in the photon flux: increased horizontal foci across the accessible bandwidth, and adequate methods to compensate for non-statistical structure arising from the scattering effects due to the nature of the samples themselves, appear to be the central issues in this respect

At the Pt L_{III}-edge, for instance, effects owing to the coherence of the source will be considerably more significant than at the Pd *K*-edge. As such, one can envisage that the removal of small-angle effects owing to the nature of the support will require a corresponding more precise matching of the reference to the sample in this respect than is required for investigation at the Pd *K*-edge.

At present, it is not, *a priori*, possible to state exactly how far the methodologies described here will be able to counter an increased susceptibility to the nature of the sample and its homogeneity that experimentation at progressively softer X-ray wavelengths using symmetrically cut Bragg polychromators will result in.

In the first instance, from a process point of view, and the following of rates of changes in XANES and EXAFS, one way forward may be to adopt a differential EXAFS approach to data collection. In such an experiment the sample at time = 0 becomes the reference for the subsequent experiment and only the changes in absorption are measured. In this experiment absolutely nothing should move, and as such the most perfect normalization should arise. This approach has been demonstrated to work well in other arenas (Pettifer *et al.*, 2005) but comes with a considerable caveat with regard to the restoration of structural data from the differential signal. Such a restoration is generally only possible for relatively simple changes (that do not, for instance, involve gross changes in coordination number/disorder parameters or types of scatterers), and wherein the detailed structure of the starting and end point are well known (for instance, through standard EXAFS experiments). It is clear that most of the sorts of changes that are occurring in working catalysts systems (amongst others) are generally of a more complex type: to the authors' knowledge, obtaining structural data in these types of situations has never been attempted using this sort of differential approach. Nonetheless, this methodology should, at least hypothetically, permit samples of the type shown in Fig. 7 to be studied at high time resolution for the kinetic investigation using EDE, if not for the structural specifics of those changes.

Beyond this the evidence would seem to suggest that methods for effectively diminishing the coherence of the source and increasing the horizontal beam size may need to be implemented to reach the point that we have achieved with the 1Pd/10ZCA catalysts, if we wish to obtain EXAFS data for samples and processes of this general type, across the full bandwidth (5–30 keV) of ID24, and with all the benefits that a transmission-based EDE experiment performed at high flux line potentially has.

As mentioned earlier, the Bonse–Hart camera configuration previously demonstrated (Hagelstein *et al.*, 1998) could form a part of such a solution from a scattering/coherence point of view and it seems likely that this will be further assessed on ID24 in the near future, as a result.

The deliberate retro-engineering (increasing) of the horizontal beam focus from its current dimensions appears to be entirely possible within the bandwidth regime where this can be foreseen to become very problematic for EXAFS studies of the type considered here ($\lesssim 15$ keV). In this respect at least one potential solution arises within the current beamline configuration: implementation of a Laue polychromator configuration. Originally demonstrated by Hagelstein (Hagelstein *et al.*, 1995; San-Miguel *et al.*, 1998), the Laue geometry has proved extremely useful, though predominantly for use at X-ray energies $\gtrsim 15$ keV [for instance, Newton, Dent, Diaz-Moreno *et al.*, 2002; Newton *et al.*, 2006*a* (Rh *K*); Hagelstein *et al.*, 1995; Ressler *et al.*, 1997 (Pd *K*); Ressler *et al.*, 2002 (Mo *K*)]. At least in part, its utility at softer energies has also been demonstrated (*e.g.* Hagelstein *et al.*, 1998; Pt L_3-

edge), though the extent to which it may be utilized at energies much below this remains to be thoroughly assessed.

As a last observation, it has generally been perceived that, along with sample uniformity issues, the greatest weakness of the dispersive approach has been the inability to make an in-line and simultaneous normalization measurement. These results show that this is not necessarily the case at all; no in-line normalization technique will account for effects owing to the very nature of the samples themselves and, as has been shown, these can be significant to the point of limitation if not accounted for. As such, a development of this nature will not, in itself, improve the situation in these terms. This being said, this sort of capacity could find utility, in respect of the sorts of studies discussed here, in accounting for, and nullifying, small but complex (for instance, apparent yawing) movements of the beam. Such residual effects have been observed on ID24 and appear to arise from tiny variations in the electron beam orbit within the synchrotron.

Beyond the immediate fields of consideration, however, it is clear that for other, increasingly important, applications of EDE, that require accumulation of data or spectra over extended periods of time (for instance, mapping experiments at high spatial resolution), the institution of a method for in-line and simultaneous normalization remains a goal of obvious utility.

5. Conclusions

Some of the limiting parameters that need to be addressed and accounted for in making a successful EDE experiment on samples prototypical of heterogeneous catalysts (and, indeed, of many other functional materials), along with the processes that they facilitate, have been addressed. In the case of supported Pd catalysts based upon Al_2O_3 and comprising differing loadings of Ce and Zr, here massive improvements in the performance of the technique can be gained through an empirical understanding of how the vertical (and by implication the horizontal) dimensions of the beam, and proper accounting for the intrinsic nature of the bulk of the sample (in this case the support material), influence the transmission experiment. Moreover, by implementing a reference that is at least as absorbing as the support material in question, we are able to utilize more of the high photon flux that ID24 supplies within the dynamic range of the 16-bit FReLoN detector. In this sense at least, the implementation of such a suitable reference means that the dispersive transmission experiment tangibly benefits from what traditional wisdom would consider a progressively more problematic situation.

It is clear that the absolute dimensions of the beam relative to the intrinsic particle size of the material plays a very important role in determining the quality of the EXAFS data obtainable.

Here we have not tested in detail the varying of the particle size of the sample itself; as pointed out earlier, what can be done in this respect is constrained by other aspects of an experiment that attempts to respect parameterization for the process under study rather than simply the criteria for obtaining good EXAFS. However, a simple quantitative guideline can be derived: the net dimensions (vertical and horizontal) of the focal point of the dispersive beam should ideally permit averaging over as large a number of particles (of a given size) as possible so as to reduce susceptibility to any spatial inhomogeneity that may exist within the system.

At the lower end of the ID24 bandwidth ($\lesssim 15$ keV), where horizontal beam foci of <10 µm are now inherent when utilizing symmetrically cut Bragg polychromators, the implications are that it is this factor that will become the greatest hurdle that needs be overcome to make the sort of measurement described here possible across this accessible bandwidth (and therefore materials) range. The Bonse–Hart configuration demonstrated by Hagelstein *et al.* (1998) is also a potential solution, in this wavelength region, to some of these issues raised here. An enlargement of the intrinsic horizontal size of the focal spot by around one order of magnitude would also appear to be required for subsecond EXAFS (rather than just XANES) to become a reality in these cases. In this respect the application of the Laue polychromator approach (Hagelstein *et al.*, 1995), to lower energy problems, may offer a way forward.

6. An additional note on the EDE specific pathlength effect and apparent limits to bed dimensions for samples and sample references

Subject to this paper having been completed, a further relevant observation has been made in the above respect. Upon testing a 4% Pd sample supported upon Al_2O_3, a significant loss of apparent energy resolution in the spectra (and a dampening of the resultant EXAFS) was noted when changing from a 5 mm pathlength to 8 mm pathlength.

In comparable solution phase studies of Pd chemistry (for instance, Guilera *et al.*, 2006), where a 10 mm pathlength is used, along with a highly absorbing/scattering fluid phase, such an effect is not observed; neither is it observed in standard EXAFS derived at powder samples at the Rh *K*- or Pd *K*-edges using the same sample presentation. As such it is concluded that this dampening effect is a result of the diffusion and scattering of the beam by (principally) the support material which is picked up in the dispersive experiment but not in the standard scanning experiment.

This means that the usual rules of calculating optimal pathlengths for a transmission EXAFS experiment have to be modified for the dispersive case in that a reduced upper limit for the transmission pathlength (and therefore the edge jump magnitude) that can be achieved without losing resolution results.

If the starting point of the experiment is known, this effect need not be fatal; although undesirable, extraction of 'real' coordination numbers is still possible by appropriately adjusting energy-resolution-related parameters in EXAFS analysis codes. It would seem far better practice, however, to empirically verify as and when this might be happening, on a system-by-system basis, by testing a variety of bed dimensions and simply optimizing to avoid this issue.

The author would like to thank Dr Trevor Mairs and Dr Sakura Pascarelli for numerous discussions regarding a variety of the issues investigated here, and particularly on achievable spot sizes in various types of Bragg and Laue polychromators. Dr Gemma Guilera, Dr Olivier Mathon, Florian Perrin, Marie-Christine Dominguez and Dr Olga Safanova are also thanked for their assistance during the course of this work. Dr Carolina Belver (Instituto de Catalisis y Petroleoquimica, Madrid, Spain) is gratefully thanked for the synthesis and provision of the Pd samples used in this work, along with Dr Marcos Fernandez-Garcia and Dr Arturo Martinez-Arias. Dr Andy Dent (Diamond Light Source, UK) is sincerely thanked for many useful discussions regarding these matters and, indeed, the initial suggestion to look more closely at the effects of vertical beam size in EDE. Lastly, the directors of the ESRF are thanked for the funding they have provided for the development of the experiments in part described here.

References

Aquilanti, G. & Pascarelli, S. (2005). *J. Phys. Condens. Matter*, **17**, 1811–1824.

Bare, S. R., Yang, N., Kelly, S. D., Mickelson, G. E. & Modica, F. S. (2007). *Catal. Today.* In the press. [doi:10.1016/j.cattod.2006.10.007.]

Baudelet, F., Odin, S, Giorgetti, C., Dartyge, E., Itie, J.-P., Polian, A., Pizzini, S., Fontaine, A. & Kappler, J.-P. (1997). *J. Phys. IV*, **7**(C2), 441–442.

Binsted, N. (1988). *PAXAS: Programme for the Analysis of X-ray Adsorption Spectra.* University of Southampton, UK.

Binsted, N. (1998). *EXCURV98.* CCLRC Daresbury Laboratory, Warrington, UK.

Bonse, U. & Hart, M. (1965). *Appl. Phys. Lett.* **7**, 238–240.

Fernández-García, M., Iglesias-Juez, A., Martínez-Arias, A., Hungria, A. B., Anderson, J. A., Conesa, J. C. & Soria, J. (2001). *Appl. Catal. B*, **31**, 39–50.

Fontaine, A., Baudelet, F., Dartyge, E. & Guay, D. (1992). *Rev. Sci. Instrum.* **63**, 960–965.

Guilera, G., Newton, M. A., Polli, C., Guino, M., Pascarelli, S. & Hii, M. (2006). *Chem. Commun.* p. 4306.

Hagelstein, M., Ferrero, C., Hatje, U., Ressler, T. & Metz, W. (1995). *J. Synchrotron Rad.* **2**, 174–180.

Hagelstein, M., Lienert, U., Ressler, T., San Miguel, A., Freund, A., Cunis, S., Schulze, C., Fontaine, A. & Hodeau, J. L. (1998). *J. Synchrotron Rad.* **5**, 753–755.

Iglesias-Juez, A., Martínez-Arias, A., Newton, M. A. & Fernández-García, M. (2004). *J. Catal.* **221**, 148–161.

Iglesias-Juez, A., Martínez-Arias, A., Newton, M. A., Fiddy, S. G. & Fernández-García, M. (2005). *Chem. Commun.* pp. 4092–4094.

Labiche, J.-C., Guilera, G., Homs, A., Mathon, O., Newton, M. A., Pascarelli, S. & Vaughan, G. (2007). In preparation.

Mathon, O., Baudelet, F., Itie, J.-P. Polian, A., d'Astuto, M., Chervin, J.-C. & Pascarelli, S. (2004). *Phys. Rev. Lett.* **93**, 255503.

Matsushita, T. & Phizackerley, R. P. (1981). *Jpn. J. Appl. Phys.* **20**, 2223–2228.

Muñoz, M., De Andrade, V., Vidal, O., Lewin, E., Pascarelli, S. & Susini, J. (2006). *Geochem. Geophys. Geosyst.* **7**, Q11020.

Newton, M. A., Belver, C., Martinez-Arias, A. & Fernandez-Garcia, M. (2007). *Nature Mater.* In the press.

Newton, M. A., Dent. A. J., Diaz-Moreno, S., Fiddy, S. G. & Evans, J. (2002). *Angew. Chem. Intl. Ed.* **41**, 2587–2589.

Newton, M. A., Dent, A. J., Diaz-Moreno, S., Fiddy, S. G., Jyoti, B. & Evans, J. (2006*a*). *Chem. Eur. J.* **12**, 1975.

Newton, M. A., Dent, A. J. & Evans, J. (2002). *Chem. Soc. Rev.* **31**, 83–95.

Newton, M. A., Dent, A. J., Fiddy, S. G., Jyoti, B. & Evans, J. (2004). *Chem. Commun.* p. 2382.

Newton, M. A., Dent, A. J., Fiddy, S. G., Jyoti, B. & Evans, J. (2006*b*). *Catal. Today* In the press. [doi:10.1016/j.cattod.2006.09.034.]

Newton, M. A., Dent, A. J., Fiddy, S. G., Jyoti, B. & Evans, J. (2007). *J. Mater. Sci.* In the press. [doi:10.1007/s10853-006-0751-y.]

Newton, M. A., Dent, A. J., Fiddy, S. G., Jyoti, B. & Evans, J. (2006*c*). *Phys. Chem. Chem. Phys.* In the press. [doi:10.1039/b613251k.]

Pascarelli, S., Mathon, O., Muñoz, M., Mairs, T. & Susini, J. (2006). *J. Synchrotron Rad.* **13**, 351–358.

Pascarelli, S., Neisius, T. & De Panfilis, S. (1999). *J. Synchrotron Rad.* **6**, 1044–1050.

Perlin, P., Jauberthie-Carillon, C., Itie, J. P., San Miguel, A., Grzegory, I. & Polian, A. (1992). *Phys Rev. B*, **45**, 83–89.

Pettifer, R. F., Mathon, O., Pascarelli, S., Cooke, M. D. & Gibbs, M. R. J. (2005). *Nature (London)*, **534**, 78–80.

Ressler, T., Hagelstein, M., Hatje, U. & Metz, W. (1997). *J. Phys. Chem. B*, **101**, 6680–6687.

Ressler, T., Weinhold, J., Jentoft, R. E. & Neisius, T. (2002). *J. Catal.* **210**, 67–83.

San-Miguel, A., Hagelstein, M., Borrel, J., Marot, G. & Renier, M. (1998). *J. Synchrotron. Rad.* **5**, 1396–1397.

Sapelkin, A. V., Bayliss, S. C., Russell., D., Clark, S. M. & Dent, A. J. (2000). *J. Synchrotron Rad.* **7**, 257–261.

Satterfield, C. N. (1996). *Heterogeneous Catalysis in Industrial Practice.* Malabar, FL: Krieger.